Gating Competence of Constitutively Open CLC-0 Mutants Revealed by the Interaction with a Small Organic Inhibitor

Sonia Traverso, Laura Elia, and Michael Pusch

Istituto di Biofisica, Sezione di Genova, CNR, Via De Marini, 6, I-16149 Genova, Italy

ABSTRACT Opening of CLC chloride channels is coupled to the translocation of the permeant anion. From the recent structure determination of bacterial CLC proteins in the closed and open configuration, a glutamate residue was hypothesized to form part of the Cl^--sensitive gate. The negatively charged side-chain of the glutamate was suggested to occlude the permeation pathway in the closed state, while opening of a single protopore of the double-pore channel would reflect mainly a movement of this side-chain toward the extracellular pore vestibule, with little rearrangement of the rest of the channel. Here we show that mutating this critical residue (Glu166) in the prototype *Torpedo* CLC-0 to alanine, serine, or lysine leads to constitutively open channels, whereas a mutation to aspartate strongly slowed down opening. Furthermore, we investigated the interaction of the small organic channel blocker p-chlorophenoxy-acetic acid (CPA) with the mutants E166A and E166S. Both mutants were strongly inhibited by CPA at negative voltages with a >200-fold larger affinity than for wild-type CLC-0 (apparent K_D at −140 mV ~4 μM). A three-state linear model with an open state, a low-affinity and a high-affinity CPA-bound state can quantitatively describe steady-state and kinetic properties of the CPA block. The parameters of the model and additional mutagenesis suggest that the high-affinity CPA-bound state is similar to the closed configuration of the protopore gate of wild-type CLC-0. In the E166A mutant the glutamate side chain that occludes the permeation pathway is absent. Thus, if gating consists only in movement of this side-chain the mutant E166A should not be able to assume a closed conformation. It may thus be that fast gating in CLC-0 is more complex than anticipated from the bacterial structures.

KEY WORDS: CLC • chloride channel • clofibric acid • chloride dependence • mutation

INTRODUCTION

The physiological relevance of CLC Cl^- channels is dramatically highlighted by their involvement in several human genetic diseases and the surprising phenotypes of mice in which the genes coding for them are deleted (for review see Jentsch et al., 2002). The determination of the three-dimensional structure of bacterial CLC homologues (Dutzler et al., 2002) marked a breakthrough of the understanding of CLC channels. Unfortunately, bacterial homologues could not be successfully studied electrophysiologically (Maduke et al., 1999). For the "prototype" *Torpedo* channel, CLC-0 (Jentsch et al., 1990), pioneering studies showed that it is functionally a dimer with two identical but independent permeation pathways (Miller and White, 1984), a model that was fully confirmed by mutagenesis (Ludewig et al., 1996; Middleton et al., 1996) and a low-resolution structure (Mindell et al., 2001), and then verified by the high-resolution structure of the bacterial StCLC (Dutzler et al., 2002). CLC channels are voltage dependent. However, the voltage dependence is not caused by the movement of a charged segment of the protein, as is the case for cation channels (Sigworth, 1994; Jiang et al., 2003a,b), but rather by the movement of a permeant anion that is accompanying channel opening in an obligate manner (Pusch et al., 1995; Chen and Miller, 1996). A highly conserved glutamate residue blocks the exit of a crystallographically resolved Cl^- ion in StCLC and Dutzler et al. (2002) proposed that the structure corresponds to a closed channel configuration and that the glutamate could be the sensor of the extracellular Cl^-. Recently Dutzler et al. (2003) succeeded in obtaining crystal structures of an *E. coli* CLC channel (EriC) in which the critical glutamate was mutated to alanine (E148A) and glutamine (E148Q). The structures of both mutants apparently represent an open channel with three closely located anion binding sites, with the outermost corresponding to the location of the negatively charged E148 side-chain in the closed channel structure. The suggestion that the structures of the mutated channels represent an open state was supported by functional data obtained with mutants of the glutamate in vertebrate CLC channels that lead to a constitutively open phenotype (Fahlke et al., 1997; Schmidt-Rose and Jentsch, 1997; Dutzler et al., 2003; Estévez et al., 2003). Thus, it appears that the single

Address correspondence to Michael Pusch, Istituto di Biofisica, Sezione di Genova, CNR, via de Marini, 6, I-16149 Genova, Italy. Fax: (139) 0106475 500; email: pusch@icb.ge.cnr.it

Abbreviation used in this paper: CPA, p-chlorophenoxy-acetic acid.

protopore gating of CLC channels involves only a very small conformational rearrangement.

In the present paper we investigated mutations of the critical glutamate and neighboring residues in the prototype *Torpedo* CLC-0 channel. In particular, we studied the block of the constitutively open mutants E166A and E166S by intracellular p-chlorophenoxy-acetic acid (CPA). The binding site of CPA and of another Cl^- channel blocker, 9-AC, was recently mapped in the muscle CLC-1 channel to a binding pocket (Estévez et al., 2003) that partially overlaps with the central Cl^- ion binding site seen in the crystal structure of EriC (Dutzler et al., 2002, 2003). The critical glutamate (E232 in CLC-1) was proposed to form part of the CPA binding site based on a tenfold increased CPA affinity of the mutant E232C (Estévez et al., 2003). Estévez et al. (2003) suggested that the identified binding pocket corresponds to a structure of the closed channel because CPA and 9-AC exhibit a strongly state-dependent block being much more potent at negative voltages, where channels are closed (Pusch et al., 2001; Accardi and Pusch, 2003; Estévez et al., 2003). However, the above mentioned, newly resolved, and presumably open bacterial CLC structures (Dutzler et al., 2003) suggest on the contrary that the open and closed conformations display only minimal structural differences.

These predictions can be tested using the small organic molecule CPA as a tool. CPA has a drastically different affinity for the closed and for the open state with the open channel block being fast and of low affinity and the closed channel block of relatively high affinity (Accardi and Pusch, 2003). It is thus a priori expected that CPA block of the constitutively open mutant E166A corresponds to the low-affinity, open-channel block of WT CLC-0. In contrast, we find that CPA exerts a strongly voltage-dependent high-affinity CPA block reminiscent of the closed state block of WT CLC-0. Further analysis of the CPA block of E166A and E166S in CLC-0 shows that these constitutively open mutants are able to assume a conformation that closely resembles the closed state of WT CLC-0 and that this conformation is strongly stabilized by CPA. This finding has important implications for the mechanism of gating of CLC-0.

MATERIALS AND METHODS

Molecular Biology and Heterologous Expression

Mutations were introduced by recombinant PCR as described (Accardi et al., 2001). All constructs were in the PTLN vector (Lorenz et al., 1996). cRNA was transcribed and injected in *Xenopus* oocytes as described (Accardi and Pusch, 2000).

Electrophysiology

Currents were recorded using the two-electrode voltage-clamp methods and excised patch-clamp recording as described (Pusch et al., 2000). For whole-oocyte voltage-clamp the bath solution contained (in mM) 100 NaCl (or 100 NaI), 4 $MgSO_4$, 5 HEPES, pH 7.3, and the holding potential was chosen close to the resting membrane potential (−30 to −50 mV). For patch-clamping, the intracellular solution contained (mM): 100 N-methyl-D-glucamine (NMDG)-Cl, 2 $MgCl_2$, 10 HEPES, 2 EGTA, pH 7.3, whereas the standard extracellular solution contained 100 NMDG-Cl, 5 $MgCl_2$, 10 HEPES, pH 7.3. In the "low Cl^-" extracellular solution 90 mM Cl^- was replaced by the impermeable glutamate. All substances were purchased from Sigma-Aldrich. CPA was applied to the internal side of the membrane by inserting the patch pipette into perfusion tubes of ~0.5-mm diameter. Patch-clamp data were recorded using an EPC-7 amplifier (HEKA) and the Pulse acquisition program (HEKA), and were analyzed using custom software. The holding potential in patch clamp measurements was 0 mV throughout.

Nonstationary Noise Analysis

Noise analysis was performed as described (Pusch et al., 1994; Saviane et al., 1999). Briefly, 50–100 identical pulses to various test potentials were applied and the mean response, I, was calculated. The variance, σ^2, was calculated from the averaged squared difference of consecutive traces. Background variance at 0 mV was subtracted and the variance-mean plot was fitted by $\sigma^2 = iI - I^2/N$, with the single channel current, i, and the number of channels, N, as free parameters. The maximal open-probability, p_{max}, was estimated by

$$p_{max} = I_{max}/(N \times i),$$

where I_{max} is the maximal current.

RESULTS

Fig. 1 A shows an alignment of the short stretch of amino acids around glutamate 166 of CLC-0 with the corresponding region of StCLC. The glutamate marks the start of helix F, whose NH_2 terminus points to the center of the channel where a Cl^- ion has been identified crystallographically (Dutzler et al., 2002). The glutamate shown in bold was mutated in CLC-0 and first studied using two-electrode voltage-clamp. For comparison, representative traces for WT CLC-0 are shown in Fig. 1 B. All mutants drastically affect gating, whereas none eliminated the characteristic block by extracellular iodide (Fig. 1, thick traces) or significantly altered the ion selectivity sequence among halides (unpublished data), indicating that the glutamate is not important for ion selectivity. Changing the glutamate to serine (unpublished data) or alanine (Fig. 1 C) completely abolished any gating relaxation, resulting in an almost linear, ohmic phenotype. In contrast, the charge-conserving E166D mutation significantly slowed channel opening (Fig. 1 D).

We concentrated on the constitutively open mutations E166A and E166S for a detailed study using the patch clamp technique. As in the whole-oocyte measurements, the open-probability of mutants E166A (Fig. 2 A) and E166S (unpublished data) was also completely insensitive to voltage in patch-clamp experi-

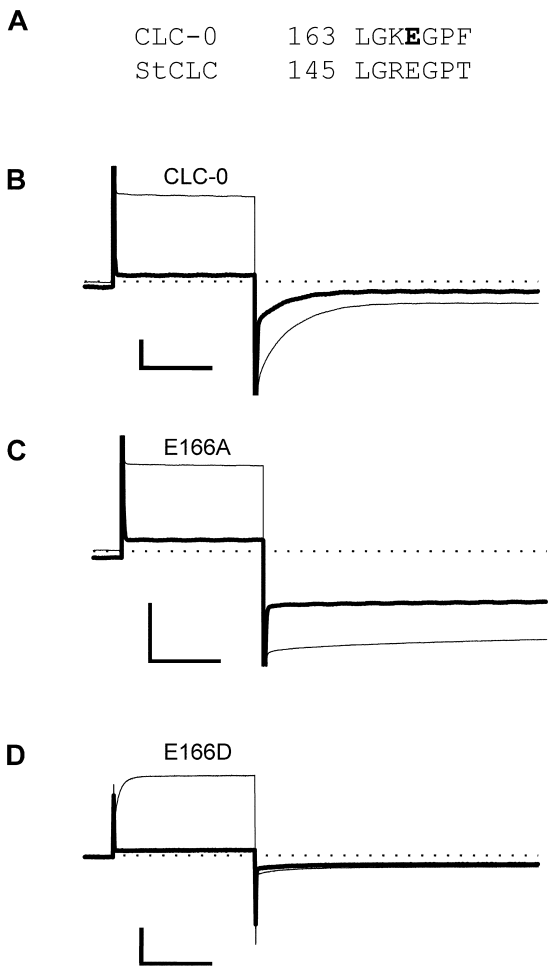

FIGURE 1. Phenotype of mutations. Glutamate 148 of the StCLC channel (Dutzler et al., 2002) marks the beginning of helix F and is part of a highly conserved structural motif of CLC channels. The phenotype of mutations E166A and E166D are illustrated in C and D. Mutant E166S (not depicted) was indistinguishable from mutant E166A, and mutant E166K (not depicted) was similar to E166A. voltage-clamp traces obtained from whole oocytes from the indicated constructs are shown. Single traces in 100 mM NaCl (thin trace) and 100 mM NaI (thick trace) measured from the same oocyte are shown superimposed. They were evoked by a pulse to 60 mV followed by a pulse to −140 mV. Horizontal bars, 50 ms. Vertical bars: 2 μA (B), 16 μA (C), 4 μA (D). Similar results were obtained for at least five oocytes for each mutant.

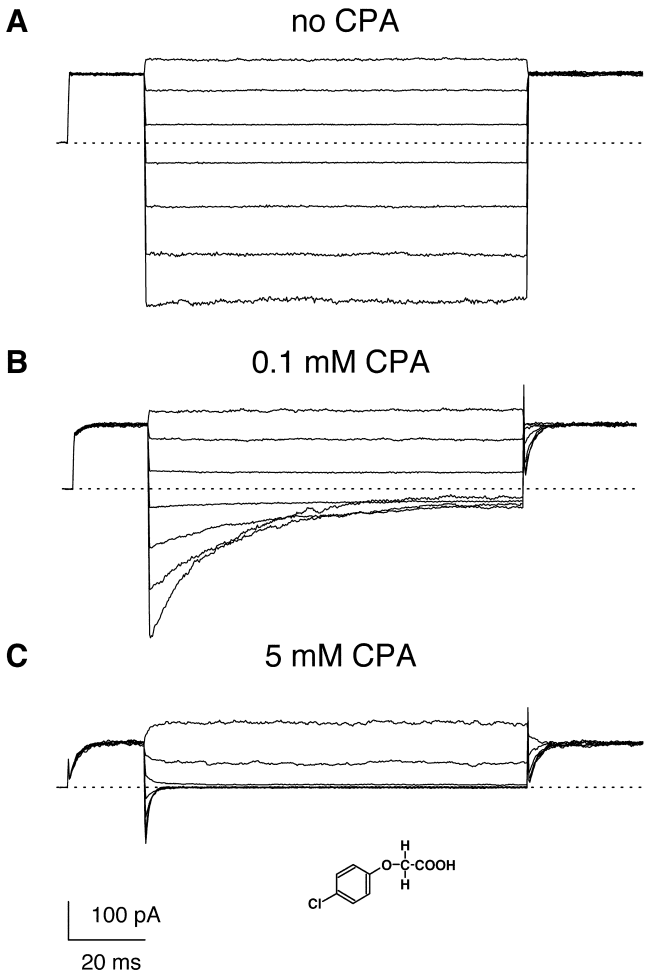

FIGURE 2. Inhibition of mutant E166A by CPA. Patch-clamp data from a representative inside-out patch are shown in the absence of CPA (A), and in the presence of 0.1 mM CPA (B) and 5 mM CPA (C). The pulse protocol consists of a prepulse to 80 mV, a test pulse to various potentials (the responses to −140, −100, −60, −20, 20, 60, and 100 mV are shown) and a "tail" pulse to 80 mV. The chemical structure of CPA is shown in C as an inset. Nearly identical results were obtained for the mutation E166S (not depicted).

ments. Furthermore, the open probability of these mutants did not depend on the extracellular or intracellular Cl^- concentration: a reduction of these to ~15 mM (reduction of $[Cl^-]_{ext}$ in two-electrode voltage clamp and of $[Cl^-]_{ext}$ or $[Cl^-]_{int}$ in excised patch clamp measurements) only shifted the current reversal potential and reduced the current amplitude (unpublished data), as expected for an open, Cl^--selective pore (Hille, 2001).

We then applied CPA (Fig. 2, inset), a known blocker of CLC-1 and CLC-0 (Accardi and Pusch, 2003; Estévez et al., 2003) to the intracellular face of the membrane (Fig. 2, B and C). CPA strongly inhibited the currents, especially at negative voltages, and the inhibition developed with concentration- and voltage-dependent kinetics. We evaluated first the steady-state inhibition as a function of the concentration of CPA ([CPA]) (Fig. 3 A). The steady-state inhibition could be well described by a simple Michaelis-Menten relationship of the form

$$I([CPA])/I(0) = 1/(1 + [CPA]/K_D^{app}), \qquad (1)$$

where I([CPA]) is the steady-state current and K_D^{app} is a voltage-dependent apparent inhibition constant (Fig. 3 A, lines). The resulting K_D^{app} values (Fig. 3 B, filled cir-

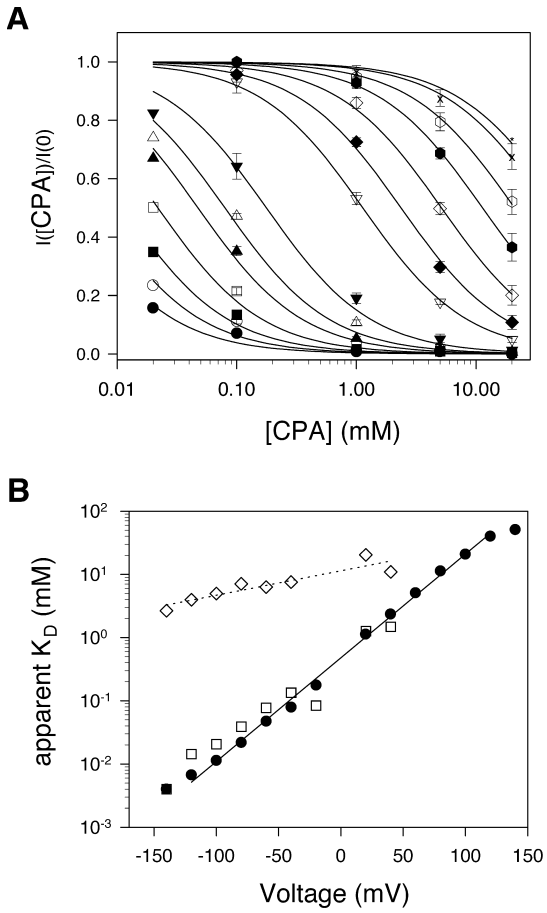

FIGURE 3. Steady-state inhibition by CPA. The inhibition seen at steady-state is shown in A as a function of [CPA] (filled circles, −140 mV; open circles, −120 mV; filled squares, −100 mV; open squares, −80 mV; filled triangles up, −60 mV, open triangles up, −40 mV; filled triangles down, −20 mV; open triangles down, 20 mV; filled diamonds, 40 mV; open diamonds, 60 mV; filled hexagon, 80 mV; open hexagon, 100 mV; cross, 120 mV; star, 140 mV). Data were obtained by averages from 5 patches. Lines in A are best fits of Eq. 1. The resulting K_D^{app} is shown in B (filled circles) as a function of voltage. The solid line represents a best exponential fit to the data from −120 to 120 mV of the form $K_D^{app}(V) = K_D^{app}(0)*\exp(z*V/(RT))$ with a valence z = 0.96 and $K_D^{app}(0) = 0.48$ mM. Diamonds represent the open channel K_D estimated by the fit of Eq. 3 to the relaxation rates shown in Fig. 8 A and the dotted line indicates an exponential function of the form $K_D(V) = K_D(0)*\exp(z_O*V/(RT))$ with $z_O = 0.23$ and $K_D(0) = 11$ mM. Open squares are calculated from Eq. 2 using the parameters obtained by fitting Eq. 3 to the relaxation rates (see Fig. 8).

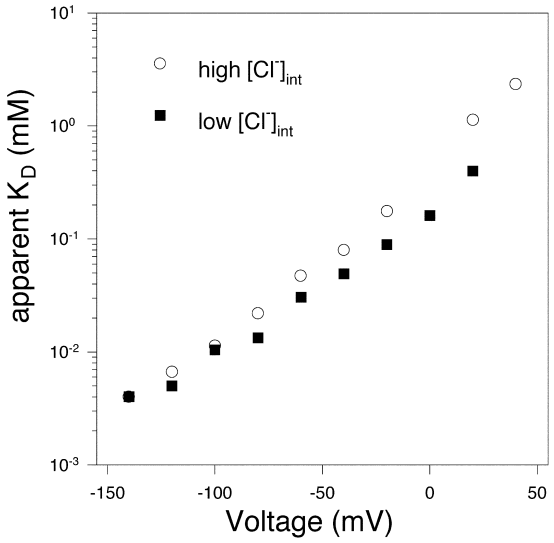

FIGURE 4. Block of E166A in low intracellular chloride. The steady-state block was evaluated using an intracellular solution in which 90 mM chloride was replaced by glutamate resulting in a solution with 14 mM Cl^- (filled squares). For comparison, the data from Fig. 3 obtained in the regular Cl^- solution are also shown (open circles). Data in low Cl^- were obtained by the average from three patches.

cles) depend on voltage in an exponential manner over four orders of magnitude with an apparent valence of 1 elementary charge (Fig. 3 B, solid line; see legend of Fig. 3). The affinity at −140 mV is ~4 μM and thus ~200-fold larger than that of CLC-0 (Accardi and Pusch, 2003; Estévez et al., 2003).

In contrast to what has been described for clofibrate block of CLC-0 (Pusch et al., 2001) the CPA block of mutant E166A was not much different at negative voltages in a solution with a lower intracellular chloride concentration, whereas for positive voltages the reduction of $[Cl^-]_{int}$ led to an increase of the apparent affinity by about a factor of three (Fig. 4).

To describe in mechanistic terms the magnitude and the kinetics of CPA block it is necessary to have a kinetic description of the channel gating in the absence of the inhibitor. The single protopore gating of WT CLC-0 channels is well described by a two-state system:

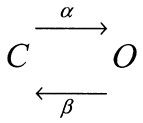

SCHEME I

with voltage-dependent opening rate-constants α and β (Hanke and Miller, 1983; Chen and Miller, 1996; Pusch et al., 2001). The lack of time, voltage, and $[Cl^-]_{ext}$ dependence of currents mediated by E166A channels could be caused by various reasons: (a) state C could be unstable (i.e., $\alpha >> \beta$); (b) α and β could have become voltage and $[Cl^-]_{ext}$ independent; (c) state C could be conducting in the mutant, with a conductance similar to that of WT or a combination of these possibilities.

The latter possibility (c) is suggested by the finding of Dutzler et al. (2002) that the glutamate residue ap-

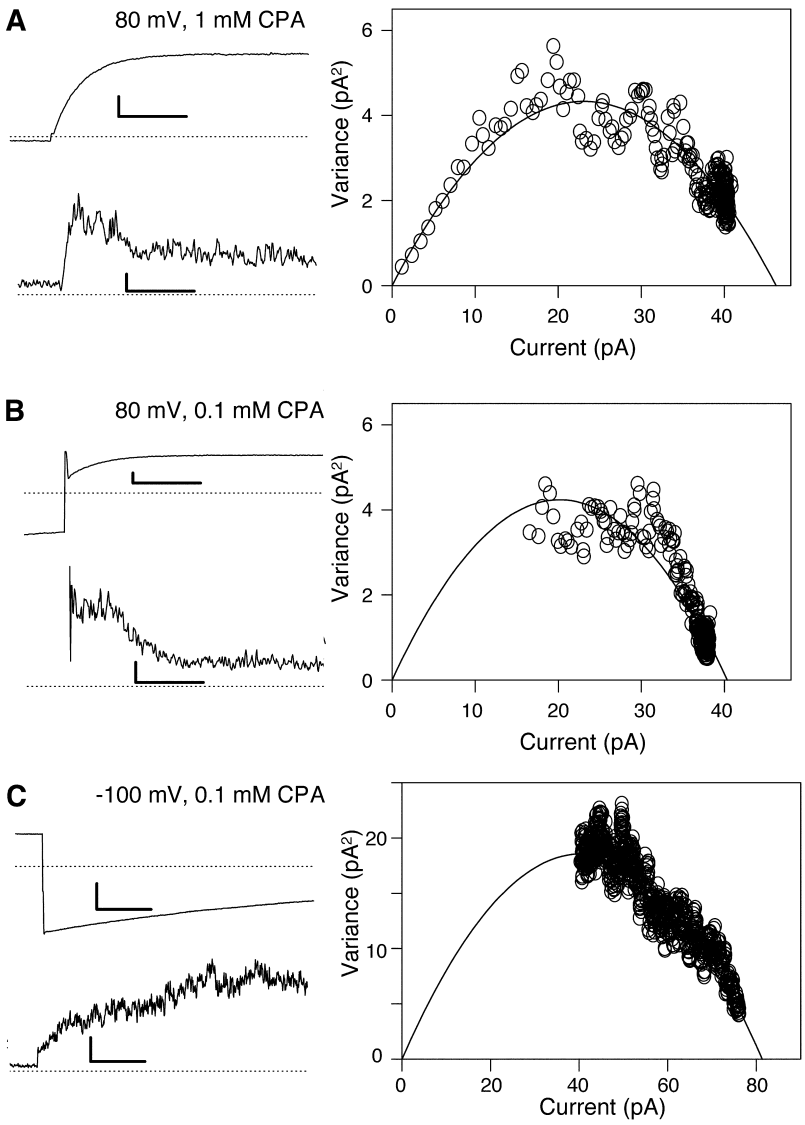

FIGURE 5. Nonstationary noise analysis of mutant E166A in the presence of CPA. Examples of nonstationary noise analysis are shown under different conditions from different patches (A, test pulse to 80 mV after a prepulse to −140 mV in the presence of 1 mM CPA; B, test pulse to 80 mV after a prepulse to −140 mV in the presence of 0.1 mM CPA; C, test pulse to −100 mV after a prepulse to 80 mV in the presence of 0.1 mM CPA). On the left are shown the mean (top trace) and the variance (bottom trace), while on the right the variance is plotted versus the mean (symbols) and fitted with a parabola (line) as described in MATERIALS AND METHODS. The parameters obtained by the fit are, A, i = 0.37 pA, N = 123, p_{max} = 0.88; B, i = 0.40 pA, N = 96, p_{max} = 0.95; C, i = 0.91, N = 89, p_{max} = 0.94. Bars: 5 ms, 10 pA, 1 pA² (A and B); 10 ms, 30 pA, 5 pA² (C). Similar results were obtained in a total of four patches.

pears to block the passage of Cl^- ions and by the hypothesis that the crystal structure of StCLC represents the closed conformation. Removing the "barrier" in the mutant could render the regular closed state a conductive open state. The recent "open" structures of mutated *E. coli* CLC (Dutzler et al., 2003) further strengthen the viability of this possibility.

The following experiments are aimed at a distinction of these three possibilities. Stationary and nonstationary noise analysis can provide substantial insight into the microscopic properties of ion channels (Conti, 1984) and recordings can be acquired at high bandwidth and with relatively ease. In particular, possibility (b) (voltage-independent α and β) can easily be tested using nonstationary noise analysis if state C remains a nonconducting closed state. In fact, if channels fluctuated between open and closed states with a certain voltage-independent open probability, $p_O = \alpha/(\alpha + \beta)$, they would generate a stationary and measurable variance of magnitude $\sigma^2 = N \times i^2 \times p_O \times (1 - p_O)$, where N is the number of channels and i the single-channel current amplitude.

For an almost constitutively open channel like E166A, nonstationary noise analysis cannot be applied in a useful manner. However, we can exploit the strong voltage dependence of the inhibition by CPA to obtain information about the open probability and the single-channel current in the absence of CPA by performing noise analysis in the presence of a small concentration of CPA. This leads to current relaxations upon voltage-steps, whereas we know that at large positive voltages only a very small steady-state inhibition is present. Such a nonstationary noise analysis is illustrated in Fig. 5 that shows the results in the presence of CPA (A, 1 mM; B and C, 0.1 mM) at 80 mV (A and B) and −100 mV (C). The left panels show the mean response (top panel) and the variance (bottom panel) calculated from several identical stimulations as described in MATERIALS

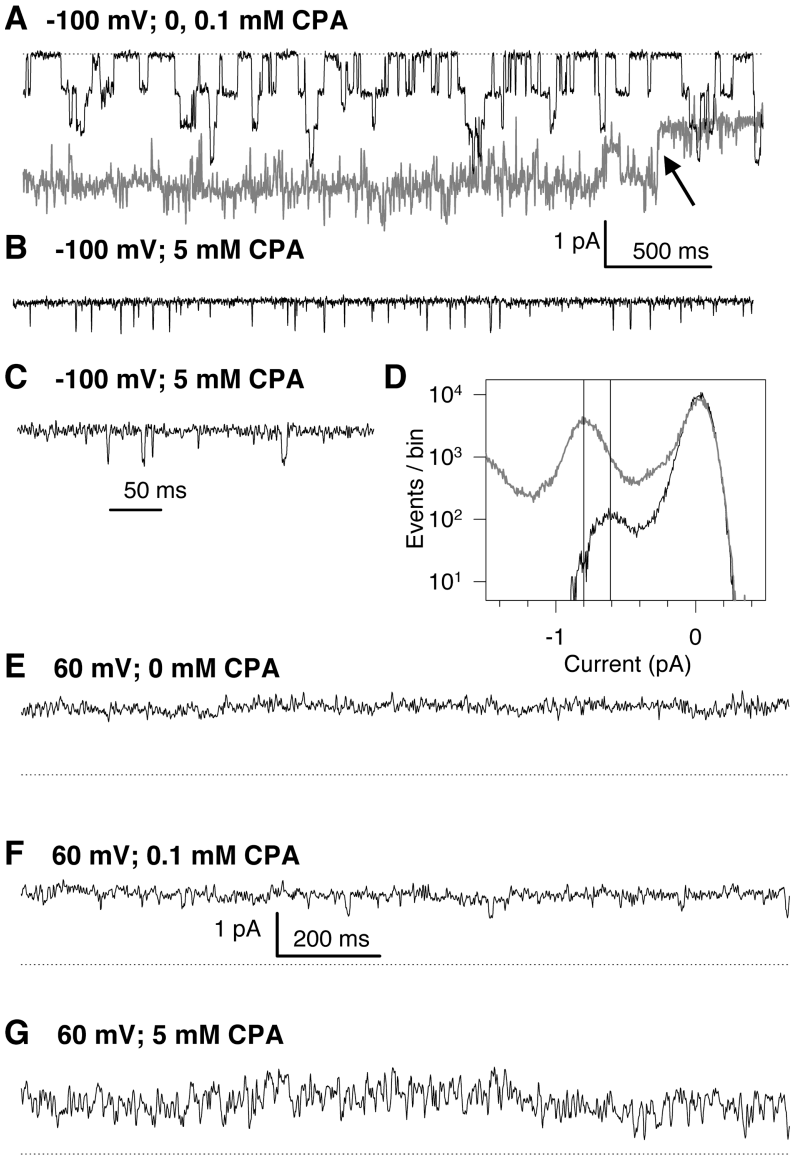

FIGURE 6. Recordings from a patch with only a few channels. Representative traces from a single patch held at −100 mV (A–C) or 60 mV (E–G) in the absence of CPA (gray trace in A and E), with 0.1 mM CPA (black trace in A and F), or 5 mM CPA (B, C, and G) are shown. In C a short stretch of the trace in B is shown at a higher time-resolution (filtered at 500 Hz, while the longer traces were filtered at 200 Hz before display). In D a raw amplitude histogram of the recording at −100 mV in the presence of 0.1 mM CPA (gray trace) and 5 mM CPA (black trace) is shown. The vertical lines are drawn at current values of −0.8 and −0.61 pA to highlight the first nonzero peaks of the respective amplitude histograms. The bin-width for the amplitude histograms was 5 fA. The vertical scale bar in A also applies to B and C, and the scale bars in F also apply to E and G. The patch most likely contained two channels with four pores. Similar results were obtained in a total of four patches.

AND METHODS. The right panels show the variance, σ^2, plotted versus the mean current, I, (symbols) together with a parabolic fit (lines) that yields estimates for the single channel current, i, the number of channels, N, and the maximal open probability, p_{max} (see MATERIALS AND METHODS). The estimated value of the single-channel current, i, at 80 mV is similar in 0.1 and 1 mM CPA (0.42 and 0.37 pA, respectively). The single-channel conductance estimated from these values and those measured at negative voltages is similar to that of WT CLC-0 (Bauer et al., 1991; Chen and Miller, 1996; Ludewig et al., 1997b; Lin et al., 1999). Most importantly, the p_{max} values at 80 mV (achieved at the end of the pulse) and also at −100 mV (corresponding to the initial points of the pulse) are close to one. For the experiments shown in Fig. 5, the values are: p_{max} = 0.88 at 80 mV with 1 mM CPA, p_{max} = 0.95 at 80 mV with 0.1 mM CPA, and p_{max} = 0.94 at −100 mV with 0.1 mM CPA. The smaller value of p_{max} in 1 mM CPA compared with that measured in 0.1 mM is in quantitative agreement with the block seen in 1 mM CPA at 80 mV that amounts to 0.07 (Fig. 3 A). Hence, an open probability of 0.88 in 1 mM CPA would scale to 0.94 in 0.1 mM CPA, almost exactly as observed experimentally. Thus, from the noise analysis an upper estimate for the probability of occurrence of a closed state, as in possibility (b), is ~5%. These considerations do not take other noise sources into account, in particular open-channel noise, a prominent feature of CLC-0 (Ludewig et al., 1997b). From the noise analysis we can practically exclude possibility (b) that the opening and closing transitions have become voltage independent and that the channel spends a significant amount of time in a closed state. Using noise analysis alone it is, however difficult to distinguish between the possibilities (a) and (c) or a combination of these with possibility (b). Schemati-

cally, possibility (a) is represented by a single kinetic state, O, whereas (c) can possibly be schematized by

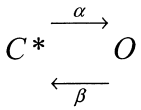

SCHEME II

where C* is a conducting state. Assuming that α and β have not completely lost their voltage dependence, the absence of macroscopic-gating relaxations in response to voltage steps excludes the possibility that that the conductance of the two states is significantly different, in agreement with the results from the noise analysis.

Additional insight into the gating behavior of E166A channels was obtained by registrations from patches that contained a small number of channels. An example is shown in Fig. 6 A, which shows superimposed traces recorded at −100 mV in the presence of 0.1 mM CPA (black trace) and without CPA (gray trace). With CPA the channels show a clear apparent gating behavior that is remarkably similar to regular single protopore gating. Without CPA the channels remain mostly in the conductive state, while occasionally gating transitions are observed, as for example at the end of the stretch illustrated in Fig. 6 A. Often, but not always, these transitions corresponded to a conductance change of about double the size of the unitary size seen with CPA (e.g., last transition of gray trace in Fig. 6 A, see arrow), and thus they probably represent gating transitions of the common gate. Even though we could not detect voltage-dependent common gate transitions using macroscopic recordings (unpublished data), it cannot be excluded that such transitions occur in a voltage-independent manner. At 5 mM CPA (Fig. 6, B and C), the overall open probability is drastically reduced and the openings at −100 mV are much shorter than those seen with 0.1 mM CPA. At this concentration the apparent conductance level of the openings was also significantly reduced compared with the ones seen with 0.1 mM CPA (Fig. 6 D). This reduction of the conductance most likely represents a fast open channel block (see below). At 60 mV the channels stay open most of the time in the absence of CPA (Fig. 6 E) and also with 0.1 mM CPA present at the intracellular side (Fig. 6 F). Occasional, slow time-scale gating transitions are seen also at 60 mV (unpublished data). Addition of 5 mM CPA leads to a flickery appearance of the current (Fig. 6 G), probably representing unresolved closure events.

The slow time base of the gating transitions seen in the absence of CPA rendered their analysis difficult. However, they are probably of little relevance to the CPA-induced effects studied here that occurred on a much faster time scale. For a further quantitative analysis we therefore relied on macroscopic current recordings that can be obtained at high-time resolution over a large voltage and concentration range.

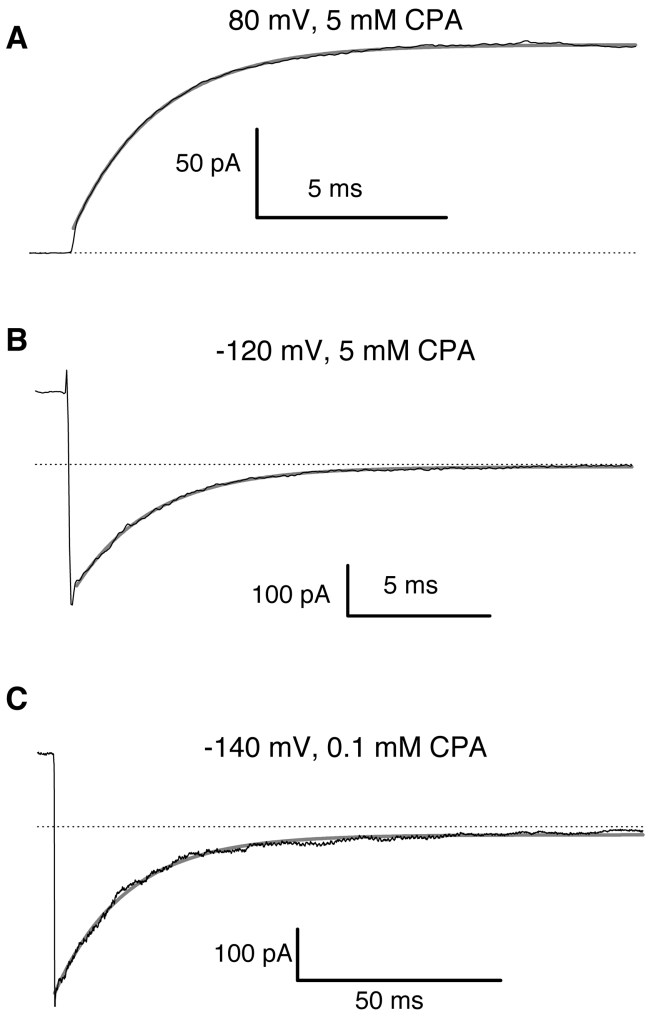

FIGURE 7. Single-exponential relaxations of mutant E166A in the presence of CPA. Examples of relaxations in the presence of CPA (A and B, 5 mM; C, 0.1 mM) at 80 mV (prepulse to −140 mV) (A), −120 mV (prepulse to 80 mV) (B), and −140 mV (prepulse to 80 mV) (C) are shown (thin lines) superimposed with single exponential fits (thick gray traces) (time constants, A, 2.2 ms; B, 2.7 ms; C, 17.5 ms).

In particular, we investigate what the minimal requirements for a quantitative description of the properties of CPA block are.

Assuming a single kinetic state, O, and considering the simplest case in which CPA is a voltage-dependent open channel blocker that binds to and dissociates from the channel with the experimentally observed kinetics, as in the scheme

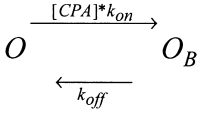

SCHEME III

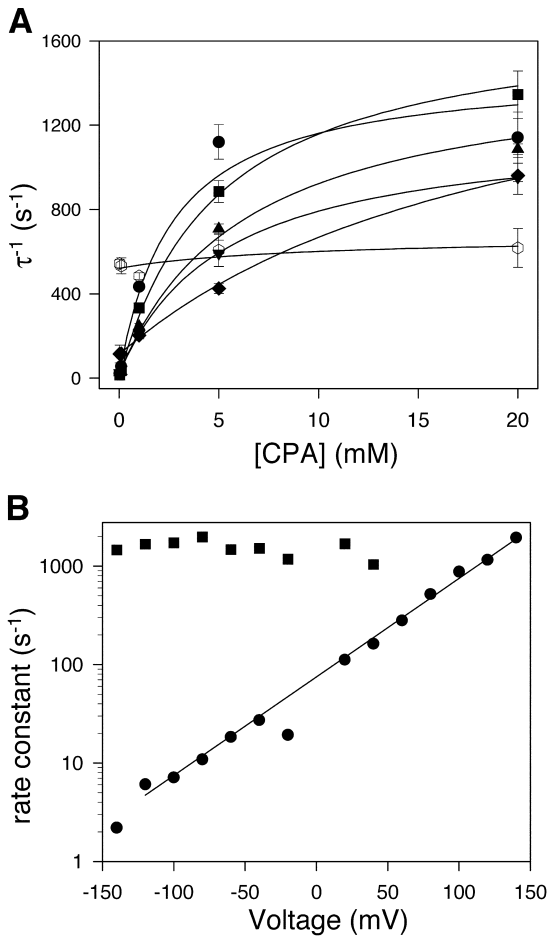

FIGURE 8. Kinetic analysis of CPA inhibition of mutant E166A. A shows relaxation rates obtained by fitting single exponential functions to the relaxations of the currents in the presence of CPA for exemplary voltages (circles, −140 mV; squares, −100 mV; triangles up, −60 mV; triangles down, −20 mV; diamond, 20 mV; open hexagons, 80 mV). Lines are fits of Eq. 3 to the data with the parameters α, β, and K_D for each voltage. In the positive voltage-range essentially only the opening rate, α, could be determined because the affinity for CPA is too low, so that the second term in Eq. 3 is small compared with α. The resulting open channel K_D is shown in Fig. 3 B (diamonds), while α (circles) and β (squares) are displayed in B as a function of voltage. The line in B is a function of the form $\alpha(V) = \alpha(0)*\exp(z_\alpha*V/(RT))$ with $z_\alpha = 0.58$ and $\alpha(0) = 75\ s^{-1}$.

the apparent K_D is the "true" open channel K_D given by $K_D = k_{off}/k_{on}$. Scheme III predicts that the relaxations observed in the presence of CPA follow a single exponential time course, in agreement with the data: relaxations could be well fitted with single exponential functions. This is illustrated in Fig. 7 that shows current relaxations (thin black traces) under various conditions (see legend of Fig. 7) superimposed with fits of a single exponential function (thick gray traces). Furthermore, Scheme III predicts that the rate, τ^{-1}, of the inhibition process is described by

$$\tau^{-1} = k_{off} + [CPA] \times k_{on},$$

i.e., τ^{-1} is a linear function of [CPA]. In contrast to this, the experimental values for τ^{-1} (Fig. 8 A, symbols) show a clear saturation at large [CPA].

To extend the simple Scheme III, and to account for the nonlinear [CPA] dependence of τ^{-1}, it is reasonable to hypothesize that drug-bound E166A channels are also able to close, in agreement with previous studies of the block of CLC-0 by CPA and related substances (Pusch et al., 2001), resulting in the extended scheme

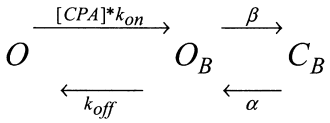

SCHEME IV

Here, drug-bound blocked channels (O_B) are able to undergo a conformational change to a closed configuration (C_B), described by the closing rate constant β and the opening rate constant α. Since the relaxations in the presence of CPA are well described by a single-exponential function and as the open channel block of CLC-0 by CPA is a fast process (Accardi and Pusch, 2003), we can suppose that CPA dissociation is much faster than the gating transitions, described by α and β. This assumption is also supported by the reduction of the apparent single channel amplitude seen with 5 mM CPA at −100 mV (Fig. 6 D). With this simplification, states O and O_B are in fast equilibrium and inhibition by CPA is characterized by an apparent dissociation constant

$$K_D^{app} = K_D/(1 + \alpha/\beta), \quad (2)$$

and the relaxation rate, τ^{-1}, depends on [CPA] as

$$\tau^{-1} = \alpha + \beta/(1 + K_D/[CPA]). \quad (3)$$

We fitted Eq. 3 to the experimental values for τ^{-1} (Fig. 8 A, lines) to estimate α, β, and the open channel K_D. Although β appears to be voltage independent (Fig. 8 B, squares), the opening rate, α (Fig. 8 B, circles), depends exponentially on voltage with an apparent valence of 0.58 (Fig. 8 B, line). The estimated open channel K_D (Fig. 3 B, diamonds) is much larger than the apparent K_D^{app} at negative voltages. As an internal check of consistency, the parameters obtained by the fit of Eq. 3 can be used to calculate K_D^{app} according to Eq. 2. The values (Fig. 3 B, open squares) are in good agreement with those found directly from the steady-state inhibition. Thus, the extended Scheme IV is able to quantitatively describe the CPA-block of mutant E166A over a large range of voltages and CPA concen-

trations. Most importantly, the parameters obtained from the fits conform with several known properties of CLC-0. For example, the open channel K_D is in the same range to what has been found for CLC-0 (Accardi and Pusch, 2003; Estévez et al., 2003). Its value is in the millimolar range and it has only a slight voltage dependence. Also the reduction of the single channel current amplitude seen in 5 mM CPA (reduction of the amplitude by 25% corresponding to an apparent K_D of 15 mM, Fig. 6 D) is qualitatively consistent with the open channel K_D of 5 mM at −100 mV found from the kinetic analysis (see Fig. 3, triangles). Even though the values differ by a factor of 3, the order of magnitude is correct and it must be kept in mind that the values in Fig. 3 for the open channel K_D have been obtained in a rather indirect way.

Furthermore, the voltage dependence of α is very similar to that of the CLC-0 protopore opening rate at positive voltages (apparent valence z = 0.58 found here compared with z = 0.7 for the Cl^--dependent component of the opening rate of CLC-0; Chen and Miller, 1996) suggesting that the opening step of CPA-bound mutant channels is analogous to the regular conformational channel opening. The analogy is not perfect as, at difference to WT gating, the closing rate constant, β, appears to be voltage independent. Altogether, Scheme IV is in very good quantitative agreement with the CPA block and results in the prediction that CPA stabilizes a conformation of the channel that corresponds to the regular closed state of WT CLC-0.

Even though Scheme IV is sufficient for a quantitative description of the CPA block it assumes inherently that the closed conformation is possible only with CPA bound and that CPA cannot bind directly to or dissociate from the closed conformation. These two properties are probably an oversimplification. Similar to what has been found for derivatives of CPA (Pusch et al., 2001) and also for CPA itself (Accardi and Pusch, 2003) a quantitative description of CPA (and CPB) block of CLC-0 pores requires the possibility that the drug binds to open and also to closed channels, though with much lower affinity and faster kinetics to the open than to the closed state. Furthermore, CPA stabilizes the closed state rendering the opening of drug-bound closed channels more difficult (Pusch et al., 2002). Adopting these findings to the gating Scheme I for E166A results in the scheme

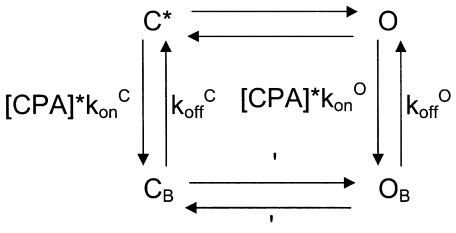

SCHEME V

with inhibition constants for the closed state $K_D^C = k_{off}^C/k_{on}^C$ and for the open state $K_D^O = k_{off}^O/k_{on}^O$. Scheme V differs from the simpler Scheme IV by the presence of the conductive state C* and it is effectively distinct from Scheme IV only if the state C* is significantly occupied. Given that Scheme V includes Scheme IV, as a special case we are certainly not able to discard it. In particular, if either α + β or k_{off}^C (or both) are much larger than α′ + β′ the scheme can be reduced to an effective three-state system

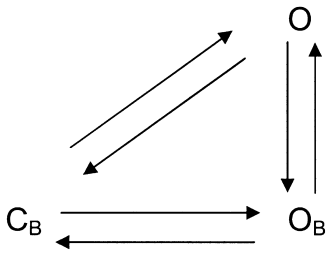

SCHEME VI

with effective rate-constants connecting states C_B and O. This scheme, which also predicts for example single exponential relaxation kinetics if the open-channel block is fast, cannot be easily distinguished from the simpler Scheme IV that lacks a direct connection between states C_B and O. However, a common feature of all these schemes that are quantitatively compatible with the data (Schemes IV–VI) is the presence of an additional state, C_B, with a relatively high CPA affinity.

As stated above, the parameters obtained by fitting Scheme IV to the kinetic data revealed a striking resemblance of the transition $C_B \leftrightarrow O_B$ to the regular CLC-0 protopore gating, suggesting that the relaxations seen in the presence of CPA at least partially reflect a conformational change that resembles regular channel gating, and that therefore state C_B is analogous to the regular closed state of WT pores.

Formally, however, Scheme IV is completely equivalent to a model in which the high-affinity state is another open state

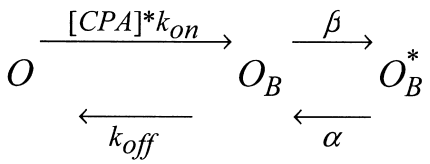

SCHEME VII

in which the rate constants α and β do not reflect a gating transition but for example a movement of CPA from a more superficial site to a deeper site.

To further test if the α-β transitions reflect regular gating transitions we changed additional parameters

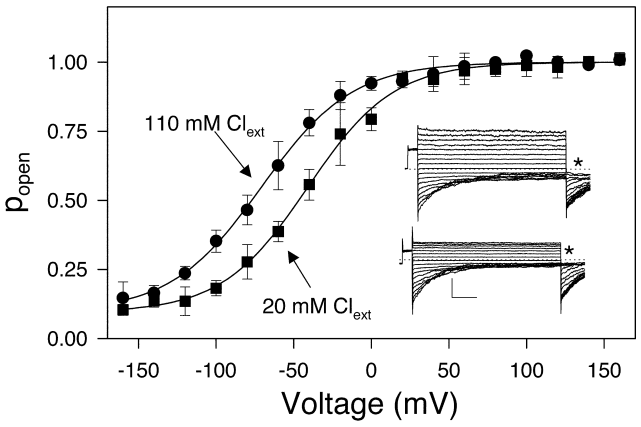

FIGURE 9. Effect of reduced $[Cl^-]_{ext}$ on CPA block of E166A. The main graph shows the open-probability as a function of voltage of E166A channels with 0.1 mM intracellular CPA in 110 mM $[Cl^-]_{ext}$ (circles) and 20 mM $[Cl^-]_{ext}$ (squares) ($n = 4$ each). The inset shows a typical family of voltage-clamp traces measured from an outside-out patch in high (top traces) and low (bottom traces) $[Cl^-]_{ext}$. The asterisk indicates the constant tail pulse at −140 mV. At 0.1 mM CPA practically no inhibition is seen at voltages >80 mV and thus the normalized initial currents at the constant "tail" pulse directly reflect the apparent open-probability at the end of a previous conditioning pulse. The normalized initial current values at this test pulse were thus used to calculate the open-probability. The lines are fits of a Boltzmann function with a voltage of half-maximal activation of −71 mV (high Cl^-) and −41 mV (low Cl^-). Scale bars in the inset indicate 50 ms and 50 pA, respectively.

that are known to interfere with fast gating of CLC-0. First, we investigated the effect of reducing the extracellular Cl^- concentration ($[Cl^-]_{ext}$) in the presence of 0.1 mM intracellular CPA. It can be seen that reducing $[Cl^-]_{ext}$ from 110 to 20 mM leads to a rightward shift of the apparent open-probability by ~30 mV (Fig. 9), similar to what is seen for the regular protopore gating of CLC-0 (Pusch et al., 1995; Chen and Miller, 1996). A similar shift might be expected, however, also for the two-open-state Scheme VI due to a direct competition with chloride.

Thus, we reasoned that if the relaxations seen in the presence of CPA reflect regular channel gating, they should be similarly affected by mutations that alter the kinetics of gating in WT CLC-0. We introduced mutations S123T and K519E, which are known to slow both the deactivation and the activation kinetics of fast gating in CLC-0 with K519E having a stronger effect (Pusch et al., 1995; Ludewig et al., 1996, 1997a). The mutations were introduced in the background of E166A and in the absence of CPA displayed a voltage-independent phenotype, however, with an outwardly rectifying current voltage relationship (unpublished data). In the presence of CPA both mutations strongly slow down the onset of and the recovery from inhibition (Fig. 10) with K519E having a larger effect.

DISCUSSION

In this work we studied CPA block of mutations of the *Torpedo* Cl^- channel CLC-0 of a highly conserved glutamate residue that has been implicated in the gating of the channel. Noncharge-conserving mutations of glutamate 166 lead to a constitutively open phenotype, as has been recently published by Dutzler et al. (2003), similarly to what happens in CLC-1 (Fahlke et al., 1997; Schmidt-Rose and Jentsch, 1997; Estévez et al., 2003). Using noise-analysis and recordings with a small number of channels we showed that the "open" phenotype of these mutations represents indeed an almost permanently conductive state, in agreement with similar findings of Dutzler et al. (2003). Infrequent gating transitions were observed for E166A that represent possible transitions of the common gate. It is, of course, difficult to definitively rule out the occurrence of closures of the regular single protopore gate. Altogether, however, the data presented here suggest that such gating transitions are practically insignificant.

In the crystal structure of the E148A mutant of the *E. coli* CLC EriC, the position of the missing negatively charged side-chain is occupied by a chloride ion while the rest of the structure is practically identical to that of the WT (Dutzler et al., 2003). Consequently, Dutzler et al. (2003) concluded that the single protopore gate mainly involves a reorientation of the Glu side-chain with almost no additional conformational change and that the alanine mutant corresponds to a permanently open channel. Here, we used the small molecule CPA as a tool to further test this hypothesis.

CPA can be used to probe gating transitions because it presents a strongly state-dependent binding. Open channel block is fast and of low affinity, while closed channels are inhibited with much higher affinity (Accardi and Pusch, 2003). CPA block of WT CLC-0 could be quantitatively described by a model similar to one that had been developed for the inhibition by the related compound CPB (Pusch et al., 2001) (Scheme V).

If the mutant E166A indeed represents a permanently open channel, its CPA-blocking properties are expected to correspond to that of the open-channel block of WT CLC-0, i.e., block should be of low-affinity, of fast kinetics, and of slight voltage dependence. The opposite was found here: CPA block is even stronger than the closed channel block of WT CLC-0, it is relatively strongly voltage dependent, and displays slow kinetics. How can this discrepancy be explained?

A linear three-state model with a fast low-affinity open-channel block and a subsequent high-affinity state could quantitatively account for the voltage and concentration dependence of steady-state inhibition and inhibition kinetics. Schemes IV and VI are formally equivalent but differ significantly in the interpretation of the transition between the two CPA-bound states. In

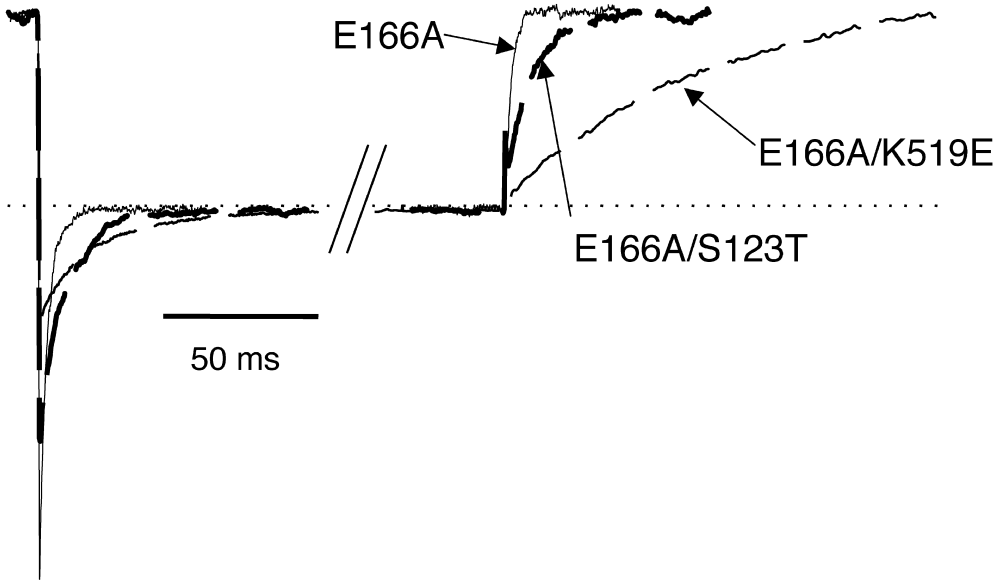

FIGURE 10. Effect of additional mutations on the kinetics of CPA block of mutant E166A. Shown are representative current traces measured with 1 mM CPA for mutant E166A (thin black trace), mutant E166A/S123T (dashed gray trace), and mutant E166A/K519E (dashed black trace). None of the mutants show any relaxation in the absence of CPA. The currents are normalized to have similar amplitude at the 80-mV prepulse, that is followed by a pulse to −140 mV, and a repolarization to 80 mV. Note also the strong outward rectification of mutant E166A/K519E, compatible with the known alterations of the open channel properties of the mutant K519E (Pusch et al., 1995; Ludewig et al., 1997a). Similar results were obtained in a total of five patches for each mutant (E166A/S123T and E166A/K519E).

Scheme IV these transitions represent a conformational change that might correspond to a closing of the channel, analogous to the block mechanism of WT CLC-0. In contrast, in Scheme VI the transition between the low- and the high-affinity states reflects a rearrangement of the CPA molecule.

For the following reasons we favor Scheme IV over Scheme VI. First, and most importantly, Scheme VI does not explain why the relaxation kinetics seen in the presence of CPA change in parallel to the normal gating kinetics when additional mutations are introduced (K519E or S123T), whereas Scheme IV naturally explains this coincidence because the relaxations seen in the presence of CPA actually reflect the regular gating. Second, no evidence for a high affinity open channel block was obtained for WT CLC-0 (Accardi and Pusch, 2003) and no evidence for two binding sites arose from the study by Estévez et al. (2003), who located the 9-AC and CPA binding site close to the central Cl^- ion binding site (Estévez et al., 2003). Lastly, the voltage dependence of the "opening" rate α is similar to that which has been described for the regular opening rate of CLC-0 (Chen and Miller, 1996). On the other hand, two other findings seemingly contradict Scheme IV: first, intracellular chloride has only a small effect on the apparent CPA affinity of the mutant, whereas the regular closing rate increases with smaller $[Cl^-]_{int}$ (Chen and Miller, 1996). Second, the "closing" rate, β, is found to be voltage independent here while the regular closing rate increases at negative voltages with an apparent valence of approximately −0.35 (Chen and Miller, 1996). In order for Scheme IV to be valid it must therefore be required that the closing transition with a bound CPA is differently sensitive to the intracellular chloride concentration and voltage compared with the regular closing rate. We believe that such a different behavior of the closing transition with a bound CPA compared with "no CPA" is not completely unexpected because it might well be that the presence of a CPA molecule inside the channel could alter the movement of chloride ions that is normally associated with channel closure and thereby alter chloride dependence and voltage dependence.

However, we cannot strictly rule out either of the two models.

Scheme IV, i.e., the ability of mutant E166A to undergo a conformational change that corresponds to a channel closure, is in contradiction to the predictions of Dutzler et al. (2003), according to which the mutant is not able to undergo a conformational closure because it lacks the relevant negatively charged side-chain of the glutamate residue. Thus, it might be that fast gating of CLC-0 involves additional conformational changes that are not revealed by the bacterial structures.

Alternatively, CPA block of E166A does not involve a conformational change as in Scheme VI. In that case the striking analogies of the transition between low- and high-affinity states to the regular gating transitions raise the suspicion that also the regular CLC-0 fast-gating kinetics do not reflect a conformational change but the movement of an ion within the channel protein.

Based on the differential effects of several pore mutations on CPA block of CLC-0 Accardi and Pusch (2003) concluded that opening of CLC-0 involves a conforma-

tional change in addition to the side-chain movement of glutamate 166, thus favoring the "conformational" Scheme IV.

We thank Alessio Accardi, Oscar Moran, and Alessandra Picollo for helpful discussions, and Mino Gaggero for the construction of the perfusion system.

This work was supported by grants from Telethon Italy (grant 1079) and the Italian Research Ministry (FIRB RBAU01PJMS). S. Traverso receives a CNR doctoral fellowship.

David C. Gadsby served as editor.

Submitted: 3 January 2003
Accepted: 21 July 2003

REFERENCES

Accardi, A., L. Ferrera, and M. Pusch. 2001. Drastic reduction of the slow gate of human muscle chloride channel (ClC-1) by mutation C277S. *J. Physiol.* 534:745–752.

Accardi, A., and M. Pusch. 2000. Fast and slow gating relaxations in the muscle chloride channel CLC-1. *J. Gen. Physiol.* 116:433–444.

Accardi, A., and M. Pusch. 2003. Conformational changes in the pore of CLC-0. *J. Gen. Physiol.* 122:277–293.

Bauer, C.K., K. Steinmeyer, J.R. Schwarz, and T.J. Jentsch. 1991. Completely functional double-barreled chloride channel expressed from a single Torpedo cDNA. *Proc. Natl. Acad. Sci. USA.* 88:11052–11056.

Chen, T.Y., and C. Miller. 1996. Nonequilibrium gating and voltage dependence of the ClC-0 Cl^- channel. *J. Gen. Physiol.* 108:237–250.

Conti, F. 1984. Noise analysis and single-channel recordings. *Curr. Top. Membr. Trans.* 22:371–405.

Dutzler, R., E.B. Campbell, M. Cadene, B.T. Chait, and R. MacKinnon. 2002. X-ray structure of a ClC chloride channel at 3.0 Å reveals the molecular basis of anion selectivity. *Nature.* 415:287–294.

Dutzler, R., E.B. Campbell, and R. MacKinnon. 2003. Gating the selectivity filter in ClC chloride channels. *Science.* 300:108–112.

Estévez, R., B.C. Schroeder, A. Accardi, T.J. Jentsch, and M. Pusch. 2003. Conservation of chloride channel structure revealed by an inhibitor binding site in ClC-1. *Neuron.* 38:47–59.

Fahlke, C., H.T. Yu, C.L. Beck, T.H. Rhodes, and A.L. George, Jr. 1997. Pore-forming segments in voltage-gated chloride channels. *Nature.* 390:529–532.

Hanke, W., and C. Miller. 1983. Single chloride channels from *Torpedo* electroplax. Activation by protons. *J. Gen. Physiol.* 82:25–45.

Hille, B. 2001. Ion Channels of Excitable Membranes. Sinauer, Sunderland, MA.

Jentsch, T.J., V. Stein, F. Weinreich, and A.A. Zdebik. 2002. Molecular structure and physiological function of chloride channels. *Physiol. Rev.* 82:503–568.

Jentsch, T.J., K. Steinmeyer, and G. Schwarz. 1990. Primary structure of *Torpedo marmorata* chloride channel isolated by expression cloning in *Xenopus* oocytes. *Nature.* 348:510–514.

Jiang, Y., A. Lee, J. Chen, V. Ruta, M. Cadene, B.T. Chait, and R. MacKinnon. 2003a. X-ray structure of a voltage-dependent K^+ channel. *Nature.* 423:33–41.

Jiang, Y., V. Ruta, J. Chen, A. Lee, and R. MacKinnon. 2003b. The principle of gating charge movement in a voltage-dependent K^+ channel. *Nature.* 423:42–48.

Lin, Y.W., C.W. Lin, and T.Y. Chen. 1999. Elimination of the slow gating of ClC-0 chloride channel by a point mutation. *J. Gen. Physiol.* 114:1–12.

Lorenz, C., M. Pusch, and T.J. Jentsch. 1996. Heteromultimeric CLC chloride channels with novel properties. *Proc. Natl. Acad. Sci. USA.* 93:13362–13366.

Ludewig, U., T.J. Jentsch, and M. Pusch. 1997a. Analysis of a protein region involved in permeation and gating of the voltage-gated Torpedo chloride channel ClC-0. *J. Physiol.* 498:691–702.

Ludewig, U., M. Pusch, and T.J. Jentsch. 1996. Two physically distinct pores in the dimeric ClC-0 chloride channel. *Nature.* 383: 340–343.

Ludewig, U., M. Pusch, and T.J. Jentsch. 1997b. Independent gating of single pores in CLC-0 chloride channels. *Biophys. J.* 73: 789–797.

Maduke, M., D.J. Pheasant, and C. Miller. 1999. High-level expression, functional reconstitution, and quaternary structure of a prokaryotic ClC-type chloride channel. *J. Gen. Physiol.* 114:713–722.

Middleton, R.E., D.J. Pheasant, and C. Miller. 1996. Homodimeric architecture of a ClC-type chloride ion channel. *Nature.* 383:337–340.

Miller, C., and M.M. White. 1984. Dimeric structure of single chloride channels from *Torpedo* electroplax. *Proc. Natl. Acad. Sci. USA.* 81:2772–2775.

Mindell, J.A., M. Maduke, C. Miller, and N. Grigorieff. 2001. Projection structure of a ClC-type chloride channel at 6.5 A resolution. *Nature.* 409:219–223.

Pusch, M., A. Accardi, A. Liantonio, L. Ferrera, A. De Luca, D.C. Camerino, and F. Conti. 2001. Mechanism of block of single protopores of the *Torpedo* chloride channel ClC-0 by 2-(p-chlorophenoxy)butyric acid (CPB). *J. Gen. Physiol.* 118:45–62.

Pusch, M., A. Accardi, A. Liantonio, P. Guida, S. Traverso, D.C. Camerino, and F. Conti. 2002. Mechanisms of block of muscle type CLC chloride channels. *Mol. Membr. Biol.* 19:285–292.

Pusch, M., A. Liantonio, L. Bertorello, A. Accardi, A. De Luca, S. Pierno, V. Tortorella, and D.C. Camerino. 2000. Pharmacological characterization of chloride channels belonging to the ClC family by the use of chiral clofibric acid derivatives. *Mol. Pharmacol.* 58:498–507.

Pusch, M., U. Ludewig, A. Rehfeldt, and T.J. Jentsch. 1995. Gating of the voltage-dependent chloride channel CIC-0 by the permeant anion. *Nature.* 373:527–531.

Pusch, M., K. Steinmeyer, and T.J. Jentsch. 1994. Low single channel conductance of the major skeletal muscle chloride channel, ClC-1. *Biophys. J.* 66:149–152.

Saviane, C., F. Conti, and M. Pusch. 1999. The muscle chloride channel ClC-1 has a double-barreled appearance that is differentially affected in dominant and recessive myotonia. *J. Gen. Physiol.* 113:457–468.

Schmidt-Rose, T., and T.J. Jentsch. 1997. Transmembrane topology of a CLC chloride channel. *Proc. Natl. Acad. Sci. USA.* 94:7633–7638.

Sigworth, F.J. 1994. Voltage gating of ion channels. *Q. Rev. Biophys.* 27:1–40.